Research Article

Busy Bursts for Trading off Throughput and Fairness in Cellular OFDMA-TDD

Birendra Ghimire,[1] Gunther Auer,[2] and Harald Haas[1, 3]

[1] Institute for Digital Communications, Joint Research Institute for Signal and Image Processing, The University of Edinburgh, EH9 3JL, UK

[2] DOCOMO Euro-Labs, Landsberger Straße 312, 80687 Munich, Germany

[3] School of Engineering and Science, Jacobs University Bremen, 28759 Bremen, Germany

Correspondence should be addressed to Harald Haas, h.haas@ed.ac.uk

Decentralised interference management for orthogonal frequency division multiple access (OFDMA) operating in time division duplex (TDD) cellular systems is addressed. Interference aware allocation of time-frequency slots is accomplished by letting receivers transmit a busy burst (BB) in a time-multiplexed minislot, upon successful reception of data. Exploiting TDD channel reciprocity, an exclusion region around a victim receiver is established, whose size is determined by a threshold parameter, known at the entire network. By adjusting this threshold parameter, the amount of cochannel interference (CCI) caused to active receivers in neighbouring cells is dynamically controlled. It is demonstrated that by tuning the interference threshold parameter, system throughput can be traded off for improving user throughput at the cell boundary, which in turn enhances fairness. Moreover, a variable BB power is proposed that allows an individual link to signal the maximum CCI it can tolerate whilst satisfying a certain quality-of-service constraint. The variable BB power variant not only alleviates the need to optimise the interference threshold parameter, but also achieves a favourable tradeoff between system throughput and fairness. Finally, link adaptation conveyed by BB signalling is proposed, where the transmission format is matched to the instantaneous channel conditions.

1. Introduction

Orthogonal frequency division multiplexing (OFDM) has been selected as a radio access technology for a number of wireless communication systems, for instance, the wireless local area network (WLAN) standard IEEE 802.11 [1], the European terrestrial video broadcasting standard DVB-T [2], and for beyond 3rd generation (B3G) mobile communication systems [3]. In OFDMA, the available resources are partitioned into time-frequency slots, also referred to as *chunks*, which can be flexibly distributed among a number of users who share the wireless medium. Provided that channel knowledge is available at the transmitter, resources can be assigned to users with favourable channel conditions, giving rise to multiuser diversity [4].

Interference management is one of the major challenges for cellular wireless systems, as transmissions in a given cell cause cochannel interference (CCI) to the neighbouring cells.

Full-frequency reuse where the transmitters are allowed an unrestricted access to all resources causes high CCI, which particularly impacts the cell-edge users [5–7]. Although CCI can be mitigated by traditional frequency planning, this potentially results in a loss in bandwidth efficiency due to insufficient spatial reuse of radio resources. Fractional frequency reuse (FFR) [4–6, 8] addresses this issue by realising that in the cellular networks CCI predominantly affects users near the cell boundary. FFR typically involves a subband with full-frequency reuse that is exempt from any slot assignment restrictions. The allocation of the remaining subbands is coordinated among neighbouring cells, in a way that the users in the given cell are denied access to subbands assigned to the cell-edge users in the adjacent cells. To this end, in [5] a user is classified as a cell-edge user based on the path loss to the desired base station (BS). This approach ignores the fact that the channel attenuation of the desired and the interfering signals is uncorrelated, and therefore fails to

exploit interference diversity. Moreover, frequency planning results in a hard spatial reuse of the available resources. As a result, it cannot cater for the dynamic traffic and load across different sites. Furthermore, in systems where BSs are dynamically added in an uncoordinated manner, such as home base stations [9], reconfigurable frequency reuse planning may prove to be increasingly cumbersome.

The busy-signal concept [10–16] has been identified as an enabler for decentralised and interference aware slot assignment. Receiver feedback informs a potential transmitter about the instantaneous CCI it causes to the "victim" receivers, which enables the transmitter to take appropriate steps to avoid interference, such as deferring its own transmission to another chunk. Early works [10, 11] rely on dedicated frequency-multiplexed channels that carry narrowband busy tones for channel reservation. As the protocol requires the transceivers to listen to the out-of-band busy tones whilst transmitting, complex RF units are required due to additional filters and duplexers involved. This drawback is avoided in [12–14], where time-multiplexed busy bursts (BBs) serve as a reservation indicator for a reservation-based medium access control (MAC) protocol. By transmitting an in-band BB in an associated minislot following a successful transmission, two important goals are accomplished [13, 14]. First, the transmitter of its own link is informed whether or not the data is successfully received. Second, at the same time potential transmitters of the competing links are notified about ongoing transmissions, so that these transmitters can take appropriate steps to avoid interference. Therefore, both slot reservation and channel sensing tasks are accomplished. Furthermore, *interference diversity* is exploited, in the way that competing links may spatially reuse the same slot, given the interfering links are sufficiently attenuated.

None of the busy tone-based MAC protocols [11–14] allow for dynamic resource allocation where multiple users share a set of parallel frequency slots of a broadband frequency-selective radio channel, such as the 100 MHz channel of the WINNER (Wireless world Initiative New Radio, www.ist-winner.org) TDD mode [17].

By extending the BB concept to OFDMA [15, 16], the channel reciprocity of TDD [18] is exploited for decentralised interference management such that the chunks can be dynamically assigned on a short-term basis thereby ensuring a soft spatial reuse of chunks among cells. This concept termed BB-OFDMA works in a completely decentralised fashion and is therefore applicable to self-organising networks, which may consist of cellular as well as *ad hoc* network topologies.

The attainable system throughput of BB-OFDMA is sensitive to the selected interference threshold [15, 16]. In this paper, it is demonstrated how the interference threshold can be tuned to tradeoff system throughput to enhance cell-edge user throughput, thereby enhancing fairness. Moreover, by using a variable BB power that takes into account the quality of the intended link, a favourable tradeoff between system throughput and fairness is achieved. A variable BB power exhibits the further advantage that the sensitivity of the selected interference threshold on the performance is mitigated. Finally, BB-OFDMA with variable BB power is the
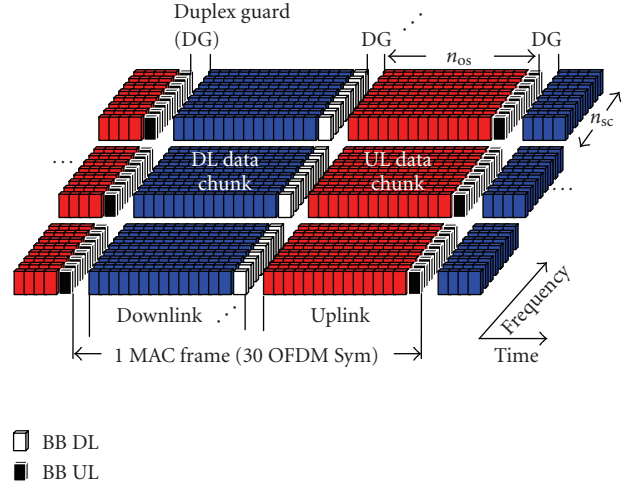

Figure 1: Frame structure for OFDMA-TDD with BB signalling.

basis for a novel receiver-driven link adaptation algorithm. System-level simulations demonstrate a significant improvement both in terms of fairness and total system throughput of BB-OFDMA, compared to the system with full-frequency reuse, where attempts to avoid interference are not made.

The remainder of the paper is arranged as follows. Section 2 describes the air interface of WINNER-TDD. The allocation of radio resources among the competing user population is discussed in Section 3. Section 4 introduces the BB signalling mechanism and its variants as well as the proposed link adaptation algorithm. The considered Manhattan grid deployment scenario and the system level simulator are introduced in Section 5, and the simulation results are discussed in Section 6. Finally, the conclusions are drawn in Section 7.

2. System Model

A time-frequency slotted OFDMA-TDD air interface based on the WINNER-TDD mode [8] is implemented, as illustrated in Figure 1. A chunk comprises of n_{sc} subcarriers and n_{os} OFDM symbols and represents a resource unit that can be allocated to one out of U users located in cell q. Successive downlink (DL) and uplink (UL) slots, each of which contains N_C chunks, constitute a frame. A chunk with frequency index $1 \leq n \leq N_C$ at frame k is denoted by (n, k). The transmit power of user v at chunk (n, k) is denoted by $T_{v,q}^d[n, k]$.

The transmitted signal of chunk (n, k) propagates through a mobile radio channel. The corresponding channel gain $G_{v,q}[n, k]$ comprises radio effects such as distance-dependent path loss, log-normal shadowing as well as channel variations due to frequency-selective fading and user mobility [19]. While channel variations of $G_{v,q}[n, k]$ between adjacent chunks in time and frequency are taken into account, fluctuations within a chunk are neglected. This approximation is justified as long as the chunk dimensions are significantly smaller than the coherence time and frequency [20].

The received signal power of user ν can be expressed as

$$\widetilde{R}_{\nu,q}^{\mathrm{d}}[n,k] = R_{\nu,q}^{\mathrm{d}}[n,k] + I_{\nu,q}^{\mathrm{d}}[n,k] + N, \tag{1}$$

where N is the thermal noise power. Both the received signal powers of the intended and the interfering links, denoted by $R_{\nu,q}^{\mathrm{d}}[n,k] = T_{\nu,q}^{\mathrm{d}}[n,k] G_{\nu,q}[n,k]$ and $I_{\nu,q}^{\mathrm{d}}[n,k]$, may vary significantly between different chunks, as elaborated in more detail in Section 4. The achieved signal-to-interference-plus-noise ratio (SINR) at chunk (n,k) is in the form

$$\gamma_{\nu,q}[n,k] = \frac{R_{\nu,q}^{\mathrm{d}}[n,k]}{I_{\nu,q}^{\mathrm{d}}[n,k] + N}. \tag{2}$$

3. Multiuser Resource Allocation

Provided that only one user per cell transmits on a given chunk, the base station (BS) may flexibly assign chunks to users, such that the intracell interference is avoided. However, as chunks may be simultaneously accessed by adjacent cells, CCI is encountered. Multiuser resource allocation is carried out by a score-based scheduler [21] variant, which distributes the $1 \leq n \leq N_{\mathrm{C}}$ chunks among $1 \leq \nu \leq U$ users served by the BS in cell q. Assuming that the channel gains $G_{\nu,q}[n,k]$ are available at BS_q, the score for user ν at chunk (n,k) is computed as

$$s_{\nu,q}[n,k] = 1 + \sum_{\ell=1}^{N_{\mathrm{C}}} \Upsilon_{\{G_{\nu,q}[n,k] \leq G_{\nu,q}[\ell,k]\}} + \epsilon_{\nu,q}[n,k], \tag{3}$$

where the Boolean operator $\Upsilon_x \in \{0,1\}$ is set to 1 or 0 when the condition x is true or false, respectively. The parameter $\epsilon_{\nu,q}[n,k] \in \{0, \infty\}$ indicates whether or not user ν is granted access to chunk (n,k). For interference aware and reservation-based MAC protocols such as BB-OFDMA (see Section 4.4), setting $\epsilon_{\nu,q}[n,k] \rightarrow \infty$ ensures that user ν in cell q is denied access to chunk (n,k). This effectively avoids radiation of CCI from cell q to any neighbouring cells that use the same chunk (n,k).

Score based multiuser scheduling with reservation assigns chunk (n,k) to user ν if either a reservation indicator was set in the previous frame, $\beta_q[n,k-1] = \nu$, or the score given by (3) is minimised

$$a_q[n,k] = \begin{cases} \arg\min_{\nu} s_{\nu,q}[n,k], & \beta_q[n,k-1] = 0, \\ \beta_{\nu,q}[n,k-1], & \text{otherwise.} \end{cases} \tag{4}$$

In case $\epsilon_{\nu,q}[n,k] \rightarrow \infty$ for all users, cell q leaves chunk (n,k) unassigned in (4). The user ν that is assigned chunk (n,k) transmits data to its intended receiver. The set of chunks $n \in \{1,\ldots,N_C\}$ at time k, for which $a_q[n,k] = \nu$ are denoted by $\mathcal{A}_{\nu,q}$. Allocated chunks $a_q[n,k] = \nu$ whose achieved SINR $\gamma_{\nu,q}[n,k]$ exceeds the target Γ, such that

$$b_q[n,k] = \begin{cases} \nu, & a_q[n,k] = \nu \text{ and } \gamma_{\nu,q}[n,k] \geq \Gamma, \\ 0, & \text{otherwise} \end{cases} \tag{5}$$

represent the set of successfully allocated chunks of user ν, denoted by $\mathcal{B}_{\nu,q} \subseteq \mathcal{A}_{\nu,q}$ [15].

For BB-OFDMA chunks with $b_q[n,k] \neq 0$ are reserved and protected from interference at the next frame $k+1$ by setting the reservation indicator to $\beta_q[n,k] = b_q[n,k]$ in (4). When the SINR target is not met, $\gamma_{\nu,q}[n,k] < \Gamma$, the reservation indicator is reset to $\beta_q[n,k] = b_q[n,k] = 0$. These chunks $\mathcal{A}_{\nu,q} \setminus \mathcal{B}_{\nu,q}$ are released in a way that user ν is prohibited access in the next slot $k+1$ by setting $\epsilon_{\nu,q}[n,k+1] \rightarrow \infty$. Subsequently, chunk $(n,k+1)$ is assigned to other users by (4).

In a cellular OFDMA system without interference protection, there is no restriction for accessing any chunks, so $\epsilon_{\nu,q}[n,k] = 0 \; \forall n,k$ in (3) for all users in the cell. Moreover, no reservation indicator is set, $\beta_q[n,k] = 0 \; \forall n,k$ in (4), irrespective of $b_q[n,k]$ in (5).

4. Busy Burst Signalling

Interference management using busy burst (BB) signalling [13, 14] establishes an exclusion region around active receivers. An exclusion region defines an area around an active receiver in cell q, where potential transmitters in adjacent cells $p \neq q$ must not transmit, so that excessive CCI by close-by interferers is mitigated. In the context of OFDMA, the exclusion regions are to be established individually for each chunk (n,k) [15]. In BB-OFDMA, an MAC frame is divided into data slots and BB minislots as illustrated in Figure 1. The BS transmits data in slot "Data DL." Provided that the SINR target for an allocated chunk (n,k) is met, the intended mobile station (MS) transmits a BB in the associated minislot "BB UL" at uplink chunk (n,k). This reserves chunk n of "Data DL" for the next frame $k+1$. Likewise, for uplink data transmitted by the MS in slot "Data UL," the BB is transmitted by the intended BS in the downlink minislot "BB DL." In summary, BB-OFDMA is described by the following protocol.

(1) All potential transmitters must sense the BB associated to the data chunk (n,k) prior to transmission.

(2) Transmitters are prohibited to access chunks where a BB is detected above a given threshold.

The resulting BB signalling overhead amounts to 6.7%, as 2 OFDM symbols out of 30 OFDM symbols per frame are used for BB signalling. However, instead of dismissing BB signalling as overhead, the BB minislots may be utilised to convey the feedback and control information. Hence, BB signalling may serve as an alternative control channel.

To exemplify the principle of BB-enabled interference avoidance in cellular system, a typical downlink and uplink interference scenario is illustrated in Figure 2. In the downlink shown in Figure 2(a), MS_1 has transmitted a BB after successful reception from BS_1. As BS_2 detects a strong BB from MS_1, BS_2 cannot spatially reuse this chunk with BS_1. In the uplink shown in Figure 2(b), BS_1 has transmitted a BB after successful reception from MS_1. While MS_2 is denied access to this chunk, as it detects a strong BB from BS_1, MS_3 is located outside the exclusion region of BS_1, and may therefore simultaneously access this chunk with MS_1.
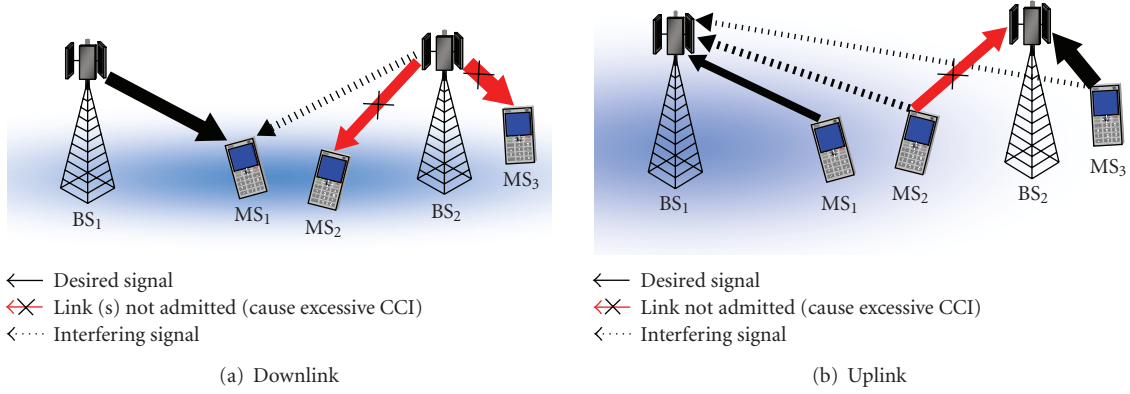
FIGURE 2: BB signalling applied to cellular system. The arrows depict the direction of desired and interfering signals and their relative strength is indicated by their width. The strength of BB signal is indicated by the darkness of the shade around the vulnerable receiver.

4.1. Two Competing Links. To mathematically describe BB-enabled interference avoidance, let $\mathbf{x} = (\nu, q)$ define a transmitter or receiver (either BS or MS) of user ν within cell q. With this notation, the channel gain of the intended link at chunk (n, k) becomes $G_{\mathbf{x}}[n, k] = G_{\nu, q}[n, k]$. The channel gain of an interfering link, between transmitter $\mathbf{y} = (\mu, p)$ of user μ located in an adjacent cell $p \neq q$ and receiver $\mathbf{x}$, is denoted by $G_{\mathbf{yx}}[n, k]$. In case two links compete for resources, the CCI between transmitter $\mathbf{y}$ and receiver $\mathbf{x}$ amounts to $I_{\mathbf{x}}^{\mathrm{d}}[n, k] = G_{\mathbf{yx}}[n, k] T_{\mathbf{y}}^{\mathrm{d}}[n, k]$. (The term $I_{\mathbf{x}}^{\mathrm{d}}[n, k]$ is equivalent to the CCI $I_{\nu, q}^{\mathrm{d}}[n, k]$ as defined in (1). While the notation $I_{\mathbf{x}}^{\mathrm{d}}[n, k]$ is preferred for intercellular interference management, the latter is used for intracell resource allocation. The same rule applies for related quantities that denote transmitted and received signal powers.) Likewise, $T_{\mathbf{x}}^{\mathrm{b}}[n, k]$ and $I_{\mathbf{y}}^{\mathrm{b}}[n, k] = G_{\mathbf{xy}}[n, k] T_{\mathbf{x}}^{\mathrm{b}}[n, k]$ are the transmit power of the BB transmitter $\mathbf{x}$ (data receiver) and the interfering BB power received at data transmitter $\mathbf{y}$ (BB receiver), respectively.

Exploiting TDD channel reciprocity [18], transmitter $\mathbf{y}$ can ascertain $I_{\mathbf{x}}^{\mathrm{d}}[n, k]$, the potential amount of interference it causes to an existing link $\mathbf{x}$, by measuring $I_{\mathbf{y}}^{\mathrm{b}}[n, k]$ at the associated BB minislot [13]. Applying the channel reciprocity property of TDD, $G_{\mathbf{yx}}[n, k] = G_{\mathbf{xy}}[n, k]$, yields

$$I_{\mathbf{x}}^{\mathrm{d}}[n, k] = I_{\mathbf{y}}^{\mathrm{b}}[n, k] \cdot \frac{T_{\mathbf{y}}^{\mathrm{d}}[n, k]}{T_{\mathbf{x}}^{\mathrm{b}}[n, k]}. \tag{6}$$

The maximum CCI $I_{\mathbf{x}}^{\mathrm{d}}[n, k]$ that a candidate transmitter $\mathbf{y}$ may cause to an active receiver $\mathbf{x}$ is determined by the interference threshold I_{th}, which is constant and known to the entire network. When $I_{\mathbf{x}}^{\mathrm{d}}[n, k] < I_{\mathrm{th}}$, transmitter $\mathbf{y}$ is located outside the exclusion range of $\mathbf{x}$. Provided that $T_{\mathbf{x}}^{\mathrm{b}}[n, k]$ is known to the candidate transmitter $\mathbf{y}$, (6) enables $\mathbf{y}$ to verify whether $I_{\mathbf{x}}^{\mathrm{d}}[n, k] < I_{\mathrm{th}}$ by invoking the threshold test [13, 14]

$$I_{\mathbf{y}}^{\mathrm{b}}[n, k] \cdot \frac{T_{\mathbf{y}}^{\mathrm{d}}[n, k]}{T_{\mathbf{x}}^{\mathrm{b}}[n, k]} \leq I_{\mathrm{th}}. \tag{7}$$

In case $T_{\mathbf{y}}^{\mathrm{d}}[n, k] = T_{\mathbf{x}}^{\mathrm{b}}[n, k]$, condition (7) reduces to

$$I_{\mathbf{y}}^{\mathrm{b}}[n, k] \leq I_{\mathrm{th}}. \tag{8}$$

By tuning I_{th}, the maximum CCI $I_{\mathbf{x}}^{\mathrm{d}}[n, k]$ in (2) is adjusted, which determines the size of the exclusion range around active receivers.

4.2. Extension to Multiple Cells. In a multicell scenario, signals from multiple links superimpose at the receiver. The total interference at data receiver $\mathbf{x}$ amounts to

$$I_{\mathbf{x}}^{\mathrm{d}}[n, k] = \sum_{\substack{\mathbf{z} \in \mathcal{T} \\ \mathbf{z} \neq \mathbf{x}}} T_{\mathbf{z}}^{\mathrm{d}}[n, k] \cdot G_{\mathbf{zx}}[n, k], \tag{9}$$

where $\mathcal{T}$ is the set of simultaneously active transmitters. Likewise, the received BB at the data transmitter (BB receiver) $\mathbf{y}$ yields

$$I_{\mathbf{y}}^{\mathrm{b}}[n, k] = \sum_{\substack{\mathbf{z} \in \mathcal{R} \\ \mathbf{z} \neq \mathbf{y}}} T_{\mathbf{z}}^{\mathrm{b}}[n, k] \cdot G_{\mathbf{zy}}[n, k], \tag{10}$$

where $\mathcal{R}$ is the set active receivers (BB transmitters).

Unlike the case when two links compete for resources, $I_{\mathbf{y}}^{\mathrm{b}}[n, k]$ is no longer equivalent to $I_{\mathbf{x}}^{\mathrm{d}}[n, k]$ in the threshold test (8). This is because in (9) the interference powers from multiple transmitters $\mathcal{T}$ add up. Consequently, the total CCI at data receiver $\mathbf{x}$ may exceed the tolerable threshold such that $I_{\mathbf{x}}^{\mathrm{d}}[n, k] > I_{\mathrm{th}}$, although the BB power (10) observed by the individual interferers $\mathbf{y} \in \mathcal{T}$ is below the threshold, $I_{\mathbf{y}}^{\mathrm{b}}[n, k] \leq I_{\mathrm{th}}$. On the other hand, in (10) the interfering BB powers from multiple simultaneously active receivers observed at $\mathbf{y} \in \mathcal{T}$ add up. It is, therefore, possible that $I_{\mathbf{y}}^{\mathrm{b}}[n, k] > I_{\mathrm{th}}$, so that link $\mathbf{y}$ is prohibited from accessing chunk (n, k), although its individual CCI contribution, $T_{\mathbf{y}}^{\mathrm{d}}[n, k] \cdot G_{\mathbf{yx}}[n, k]$ would be below I_{th}. Note that the former effect partly compensates the latter. Moreover, in many cases the interference is dominated by one strong interfering source. Therefore, the threshold test (8) provides a good approximation to the level of interference potentially caused to the active receivers.

4.3. Initial Access in Contention. Initial access of unreserved slots in BB-OFDMA is carried out in contention. During contention, two or more transmitters from adjacent cells may access chunk (n,k) simultaneously. As a result, one or several links may encounter a collision on chunk (n,k), where the SINR target is not met. To reduce the occurrence of simultaneously accessed chunks in contention, a p-persistent chunk allocation procedure is applied to BB-OFDMA, where chunk (n,k) in cell q is accessed with probability p. Denoting the outcome of the p-persistent chunk allocation with the binary random variable $\chi_q[n,k] \in \{0,1\}$, the access probability yields $P(\chi_q[n,k] = 1) = p$. The impact of p on the system performance is investigated in Section 6.1.

4.4. Decentralised Chunk Reservation with BB Signalling. The BB-OFDMA protocol enables a link $\mathbf{x} = (\nu,q)$ to contend for a chunk once it is ensured that the CCI caused to the coexisting links $\mathbf{y}$ in the neighbouring cells is below a given threshold (8). Prior to accessing chunk (n,k), transmitter $\mathbf{x} = (\nu,q)$ listens to the associated BB minislot. Whether a user ν within cell q may contend for chunk (n,k) in (4) is controlled by

$$\epsilon_{\nu,q}[n,k] = \begin{cases} 0, & I_{\nu,q}^b[n,k] \leq I_{th} \text{ and } \chi_q[n,k] = 1, \\ \infty, & \text{otherwise.} \end{cases} \quad (11)$$

Chunks, where $a_q[n,k] = \nu$ in (4), are allocated to user ν. Those chunks where the achieved SINR is above a required SINR target, $\gamma_{\nu,q}[n,k] \geq \Gamma$, are reserved by setting the reservation indicator $\beta_q[n,k] = \nu$ in (4), and are subsequently protected from CCI by BB broadcast. The BB broadcast from the intended data receiver is observed as a *surge* in the received BB power [14], which effectively notifies the transmitter that the data of chunk (n,k) has been correctly received. User ν then reserves chunk n in the next frame $k+1$ by setting $b_q[n,k+1] = \nu$ in (5). On the other hand, if the transmitter does not detect a BB surge, it is understood that the SINR target was not met due to high CCI. These chunks are released by a reset of the reservation indicator to $\beta_q[n,k] = 0$ and setting $\epsilon_{\nu,q}[n,k] \to \infty$, so that chunk $(n,k+1)$ may be assigned to other users.

4.5. Balancing System Throughput and Fairness. Cell-edge users are particularly affected by CCI for two reasons. First, the desired signal levels $R_{\mathbf{x}}^d[n,k]$ are, on average, much weaker compared to users in close vicinity to the desired BS due to relatively low channel gains on their intended links $G_{\mathbf{x}}[n,k]$. Second, cell-edge users suffer from high CCI in the downlink, or cause high CCI to the adjacent cells in the uplink.

By tuning the interference threshold I_{th} in (8), the amount of CCI $I_{\mathbf{x}}^d[n,k]$ caused to the receiver of a preestablished and coexisting link $\mathbf{x} = (\nu,q)$ is adjusted. Lowering I_{th} enforces a larger exclusion region around a vulnerable receiver. This enables cell-edge users to meet their SINR target Γ with a greater likelihood. On the other hand, by augmenting I_{th}, the number of simultaneously served links increases, giving rise to an enhanced system throughput.

However, the cell-edge users are less likely to maintain their SINR target as interference protection is gradually eliminated. The chunks are released where the SINR target is not met, which means that these chunks are no longer reserved. Since the cell-centre users are less exposed to CCI, the chunks released by the cell-edge users are likely to be reallocated to the cell-centre users. As the allocation of the resources is shifted from the cell-edge users towards the cell-centre users, fairness is compromised. Hence, by adjusting I_{th}, system throughput is traded off for fairness.

A common measure to quantify fairness is Jain's fairness index [22], defined by

$$F = \frac{\left| \sum_{\nu=1}^{U} \left| \mathcal{B}_{\nu,q} \right| \right|^2}{U \sum_{\nu=1}^{U} \left| \mathcal{B}_{\nu,q} \right|^2}, \quad (12)$$

where U is the number of users in a given cell q. The user throughput $|\mathcal{B}_{\nu,q}|$ accounts for the number of successfully transmitted/received bits by user ν, as defined in (5). A fairness index of $F = 1$ represents a perfectly fair system where all users achieve the same throughput. On the other extreme, a fairness index of $1/U$ represents an unfair system where one user is served while all other users starve. We note that the fairness definition (12) is a relative measure, which ignores the absolute achieved throughput per user. To this end, a good fairness index F may coincide with poor spectrum utilisation. For instance, a system where two users achieve 1 Mbps and 2 Mbps would result in a poorer fairness index than a system where both users achieve only 0.5 Mbps. When analysing fairness, the fairness definition (12) should therefore be considered jointly with user throughput results.

(1) Consequences for the Downlink. In the downlink, MSs at the cell edge are exposed to high CCI from transmitters in adjacent cells (see Figure 2(a)). Note that the CCI observed at a given cell (cell 1 in Figure 2(a)) is independent of the user distribution in adjacent cells (cell 2 in Figure 2(a)), assuming a constant transmit power $T_{\mathbf{x}}^d[n,k]$. This implies that if BS_2 lies within the exclusion region of MS_1, resources reserved by MS_1 cannot be spatially reused by *any* of the links in cell 2. However, if I_{th} is increased such that BS_2 is located outside the exclusion region of MS_1, *all* links in cell 2 qualify for a spatial reuse of the resources reserved by MS_1. However, the SINR target at MS_1 is less likely to be met. Should the SINR target at MS_1 not be met, this would cause the chunk allocated to MS_1 to be released and reallocated to another user served by BS_1- possibly a user that is located closer to the the serving BS_1. Therefore, the cell-edge throughput would suffer.

(2) Consequences for the Uplink. In the uplink, the transmitters (MSs) are distributed uniformly over the coverage area of the BS (see Figure 2(b)). Unlike the downlink, the CCI at the tagged BS depends on which MS transmits in the adjacent cell. To this end, the CCI observed at BS_1 in Figure 2(b) depends on whether MS_2 or MS_3 transmits to BS_2. Suppose that in cell 2 both MS_2 and MS_3 contend with MS_1 in cell 1 for chunks (n,k) and (n',k). In case MS_2 and
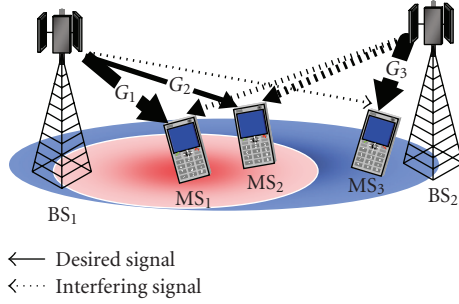
FIGURE 3: Busy burst with interference tolerance signalling (BB-ITS) in the downlink. The ovals represent the exclusion region formed with BB-ITS.

MS_1 simultaneously access chunk (n, k), while MS_3 and MS_1 simultaneously access chunk (n', k), the SINR at BS_1 tends to be superior on chunk (n', k) due to the lower CCI caused by MS_3. While MS_2 causes excessive CCI to BS_1, MS_1 and MS_3 may share chunk (n', k), although both users might be located near the cell boundary. Thus the uplink benefits from *interference diversity* due to the distributed location of mobile users. As a result, the degradation of performance at the cell edge at high I_{th} in uplink mode is less severe compared to the downlink.

4.6. Interference Tolerance Signalling via Busy Bursts. With fixed power BB signalling, the same level of interference protection is given to all links, disregarding the quality of the intended link. In case two receivers MS_1 and MS_2 with respective channel gains $G_1 > G_2$ are exposed to the same interference, as illustrated in Figure 3, the SINR target Γ is more likely met for MS_1 than for MS_2. By allowing MS_1 and MS_2 to transmit a BB with variable power, the individual amount of interference that can be tolerated by MS_1 and MS_2 is signalled to candidate transmitters in adjacent cells. Exclusion regions of different size are effectively formed around MS_1 and MS_2, as illustrated in Figure 3.

For busy burst with interference tolerance signalling (BB-ITS), the objective is that a given SINR target, $\gamma_{\mathbf{x}}[n, k] \geq \Gamma$, is maintained for an active receiver $\mathbf{x}$. This means that the maximum allowable interference depends on the intended link quality $R_{\mathbf{x}}^{\mathrm{d}}[n, k]$. Let $I_{\mathbf{x}}^{\mathrm{tol}}[n, k]$ denote the interference limit, for which the SINR (2) approaches $\gamma_{\mathbf{x}}[n, k] = \Gamma$. Then the tolerable interference at receiver $\mathbf{x}$ is upper bounded by

$$I_{\mathbf{x}}^{\mathrm{d}}[n, k] \leq I_{\mathbf{x}}^{\mathrm{tol}}[n, k] = \frac{R_{\mathbf{x}}^{\mathrm{d}}[n, k]}{\Gamma} - N. \quad (13)$$

Adjusting the tolerable interference level (13) implies that larger exclusion regions are formed for links with weak desired signal levels $R_{\mathbf{x}}^{\mathrm{d}}[n, k]$ and vice versa.

To signal the variable interference tolerance level $I_{\mathbf{x}}^{\mathrm{tol}}[n, k]$ of a victim receiver $\mathbf{x}$ to candidate transmitters $\mathbf{y}$ in adjacent cells, the BB transmit power $T_{\mathbf{x}}^{\mathrm{b}}[n, k]$ is adjusted, such that the simple threshold test $I_{\mathbf{y}}^{\mathrm{b}}[n, k] \leq I_{th}$ in (8) is retained. Hence no additional information for channel sensing is required for BB-ITS. The received BB power approaches a fixed threshold, $I_{\mathbf{y}}^{\mathrm{b}}[n, k] = I_{th}$, if the CCI approaches

$I_{\mathbf{x}}^{\mathrm{d}}[n, k] = I_{\mathbf{x}}^{\mathrm{tol}}[n, k]$. Inserting $I_{\mathbf{x}}^{\mathrm{d}}[n, k] = I_{\mathbf{x}}^{\mathrm{tol}}[n, k]$ and $I_{\mathbf{y}}^{\mathrm{b}}[n, k] = I_{th}$ into (6) yields the variable BB power $T_{\mathbf{x}}^{\mathrm{b}}[n, k] = T_{\mathbf{y}}^{\mathrm{d}}[n, k] \cdot I_{th}/I_{\mathbf{x}}^{\mathrm{tol}}[n, k]$. Assuming that $T_{\mathbf{y}}^{\mathrm{d}}[n, k]$ is fixed and denoted by T^{d}, the BB transmit power is adjusted as follows [23]:

$$T_{\mathbf{y}}^{\mathrm{b}}[n, k] = \min\left(\frac{I_{th} \cdot T^{\mathrm{d}}}{R_{\mathbf{x}}^{\mathrm{d}}[n, k]/\Gamma - N}, T_{\max}^{\mathrm{b}}\right), \quad (14)$$

where $T_{\max}^{\mathrm{b}}$ is the maximum BB transmit power. The min operator ensures that $T_{\mathbf{x}}^{\mathrm{b}}[n, k] \leq T_{\max}^{\mathrm{b}}$. Note that when $R_{\mathbf{x}}^{\mathrm{d}}[n, k]/\Gamma < N$, we get $\gamma_{\mathbf{x}}[n, k] < \Gamma$. In this situation, the chunk is released and no BB is transmitted. Therefore, it is ensured that $T_{\mathbf{x}}^{\mathrm{b}}[n, k]$ in (14) always has a positive value. We note that $I_{\mathbf{x}}^{\mathrm{b}}[n, k] = T_{\mathbf{y}}^{\mathrm{b}}[n, k] \cdot G_{\mathbf{xy}}[n, k]$ and $T_{\max}^{\mathrm{b}} = T_{\mathbf{y}}^{\mathrm{d}}[n, k] = T_{\mathbf{x}}^{\mathrm{d}}[n, k]$. It can be checked by plugging (14) into (8) that the threshold test (8) effectively checks if $I_{\mathbf{y}}^{\mathrm{d}}[n, k] \leq I_{\mathbf{y}}^{\mathrm{tol}}[n, k]$, regardless of the threshold used, as long as the BB transmit power is not clipped. In this paper, we choose $I_{th} = -90$ dBm because the probability of BB transmit power being clipped was found to be lower than 0.05 for the given deployment scenario with $\Gamma = 11.3$ dB used. Furthermore, with this threshold, the received BB at the intended transmitter (the lower bound of which is approximated by $I_{th} \cdot \Gamma$) remains well above the noise floor -117.8 dBm, such that it can be reliably detected.

4.7. Link Adaptation with BB Signalling. Receiver feedback based on BB-ITS (see Section 4.6) allows for receiver-driven link adaptation, where the chosen transmission rate is adapted to the instantaneous channel conditions. Let $\mathcal{M} = \{1, \dots, M\}$ be the set of supported modulation schemes. Associated to each modulation scheme $m \in M$ is an SINR target $\Gamma = \Gamma_m$ that must be achieved to satisfy a given frame error rate (FER).

Provided that the channel response does not change between successive frames, changes in Γ_m may be signalled from receiver to transmitter through (14), since any fluctuation in received BB power $R_{\mathbf{x}}^{\mathrm{b}}[n, k] = G_{\mathbf{x}}[n, k] T_{\mathbf{x}}^{\mathrm{b}}[n, k]$ is due to a change of Γ_m in (14). In summary, BB-ITS serves two important objectives. First, by adjusting the SINR target Γ_m, the receiver implicitly signals to the transmitter through BB-ITS that the transmission format should be changed; second, by varying the BB power $T_{\mathbf{x}}^{\mathrm{b}}[n, k]$ in (14), the size of the exclusion region around the active receiver is adjusted, so that the required SINR target Γ_m is met in successive frames.

Link adaptation with BB-ITS is carried out in two phases: the *contention phase,* where the link is established and the *link adaptation* (LA) phase, where the receiver adjusts its transmission format to the current channel conditions.

Contention Phase. In contention, multiuser chunk allocation is carried out as described in Section 4.3. To contend for an unreserved chunk (n, k), transmitter $\mathbf{x} = (\nu, q)$ initially uses the modulation scheme with the lowest spectral efficiency $m_{\mathbf{x}}[n, k] = 1$. Chunks that satisfy $\gamma_{\mathbf{x}}[n, k] \geq \Gamma_1$ are reserved in the next frame $k + 1$ by BB signalling (see Section 4.4), where the transmit power $T_{\mathbf{x}}^{\mathrm{b}}[n, k]$ in (14) is set using $\Gamma = \Gamma_1$. Then the transmission proceeds to the link adaptation phase.

Link Adaptation Phase. The objective of the link adaptation phase is to select the modulation scheme $m_{\mathbf{x}}[n,k] \in \mathcal{M}$ for chunk (n,k), which yields the highest spectral efficiency, for which $\gamma_{\mathbf{x}}[n,k] \geq \Gamma_{m_{\mathbf{x}}[n,k]}$ holds. By utilising BB-ITS link, adaptation is accomplished without any explicit feedback. The receiver executes the following algorithm.

(1) Calculate the achieved SINR $\gamma_{\mathbf{x}}[n,k]$ at chunk (n,k).

(2) Increment the number of bits per symbol based on $\gamma_{\mathbf{x}}[n,k]$

$$m_{\mathbf{x}}[n,k+1] = \begin{cases} m_{\mathbf{x}}[n,k] + 1, & \gamma_{\mathbf{x}}[n,k] \geq \Gamma_{m_{\mathbf{x}}[n,k]+1}, \\ & m_{\mathbf{x}}[n,k] < M, \\ m_{\mathbf{x}}[n,k] - 1, & \gamma_{\mathbf{x}}[n,k] < \Gamma_{m_{\mathbf{x}}[n,k]}, \\ m_{\mathbf{x}}[n,k], & \text{otherwise.} \end{cases} \quad (15)$$

(3) If $m_{\mathbf{x}}[n,k+1] \geq 1$, adjust the BB power (14) using the SINR target $\Gamma = \Gamma_{m_{\mathbf{x}}[n,k+1]}$ and transmit the BB.

(4) If $m_{\mathbf{x}}[n,k+1] < 1$, terminate the link adaptation phase and return to the contention phase.

The transmitter senses the BB minislot associated to chunk (n,k). In order to determine the modulation scheme $m_{\mathbf{x}}[n,k+1]$ requested by the receiver, the transmitter executes the following algorithm.

(1) Measure the busy signal power received from the intended data receiver $R_{\mathbf{x}}^{\mathrm{b}}[n,k]$ and compute the difference to the BB power received from intended data receiver in the preceding slot, $\Delta R = R_{\mathbf{x}}^{\mathrm{b}}[n,k] - R_{\mathbf{x}}^{\mathrm{b}}[n,k-1]$.

(2) The modulation format is adjusted based on ΔR as follows:

$$\hat{m}_{\mathbf{x}}[n,k+1] = \begin{cases} \hat{m}_{\mathbf{x}}[n,k] + 1, & \Delta R \geq I_{\mathrm{th}} \Delta \Gamma_m - \varepsilon, \\ \hat{m}_{\mathbf{x}}[n,k] - 1, & \Delta R < I_{\mathrm{th}} \Delta \Gamma_{m-1} + \varepsilon, \\ \hat{m}_{\mathbf{x}}[n,k], & \text{otherwise,} \end{cases} \quad (16)$$

where $\Delta \Gamma_m = \Gamma_m - \Gamma_{m+1}$, $m = \hat{m}_{\mathbf{x}}[n,k]$. The constant $\varepsilon > 0$ introduces a detection margin to enhance the robustness towards estimation errors in $\hat{R}_{\mathbf{x}}^{\mathrm{b}}[n,k]$ due to channel variations and noise.

(3) If $\hat{m}_{\mathbf{x}}[n,k+1] \geq 1$, transmit data on chunk $(n,k+1)$ using the new modulation scheme $\hat{m}_{\mathbf{x}}[n,k+1]$.

(4) If $\hat{m}_{\mathbf{x}}[n,k+1] < 1$, terminate the link adaptation phase and return to the contention phase.

Estimation errors due to channel variations and noise may cause detection errors, so that $\hat{m}_{\mathbf{x}}[n,k] \neq m_{\mathbf{x}}[n,k]$. Mismatch between the selected modulation schemes at transmitter and receiver can be mitigated if the transmitter announces $\hat{m}_{\mathbf{x}}[n,k]$ together with payload data on chunk (n,k).
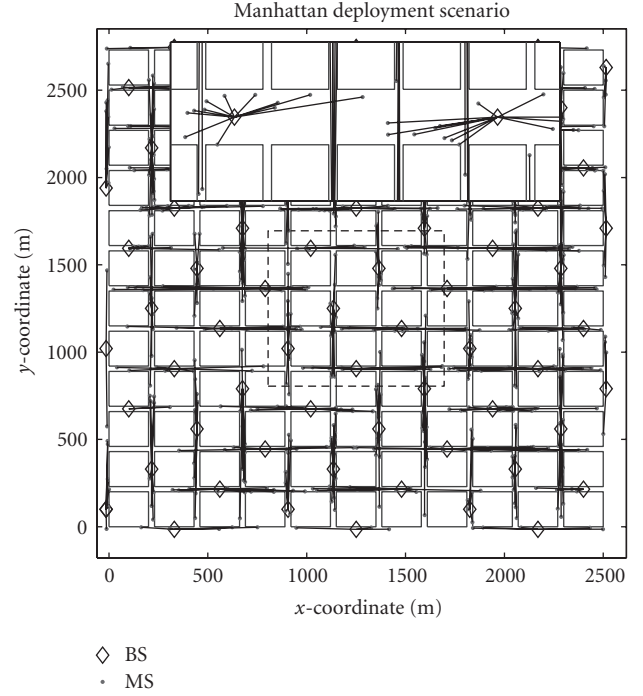

FIGURE 4: Manhattan grid urban microcell deployment.

4.8. Benchmark System. Full-frequency reuse with adaptive score-based chunk allocation (ASCA) is considered as the benchmark system. This means that neither chunk reservation nor interference avoidance mechanisms is in place. In order to maintain a fair comparison, the same fair scheduling algorithm (3) as in BB-OFDMA is applied. With ASCA, the score-based scheduler assigns chunk (n,k) to user ν whose score (3) is minimised

$$a_q[n,k] = \arg\min_{\nu} s_{\nu,q}[n,k]. \quad (17)$$

Chunk allocation for ASCA (17) corresponds to (4) by setting the reservation indicator to zero, $\beta_q[n,k] = 0$, and by allowing a cell to access all chunks, which is achieved by setting $\epsilon_{\nu,q}[n,k] = 0$ for all n,k in (3).

5. Manhattan Grid Deployment

An urban microcell deployment with a rectangular grid of streets (Manhattan grid) as defined in scenario B1 in WINNER [17] is considered, where antennas are mounted below the rooftop. The deployment scenario consists of building blocks of dimensions $200\,\text{m} \times 200\,\text{m}$, interlaced with the streets of width $30\,\text{m}$, forming a regular structure called the Manhattan grid, as shown in Figure 4. The network consists of 11×12 building blocks (72 BSs). However, the performance statistics are collected only over the central core of 3×3 building blocks (6 BSs), so as to reduce edge effects.

On average $U = 10$ MSs are served by one cell, uniformly distributed in the streets and moving with a constant velocity of $5\,\text{km/h}$. BSs are placed in the middle of the street canyons with an inter-BS distance of 4 building blocks, as

depicted in Figure 4. Distance dependent path loss, log-normal shadowing, and frequency selective fading are taken into account, as specified in [24], channel model B1. While the effect of user mobility on the channel response due to the Doppler effect is taken into account, movement of users along the streets is not considered during the duration of one snapshot. Links where transmitter and receiver are located on the same street are modelled as line-of-sight (LoS) channels, with significantly lower path loss attenuation than nonline-of-sight (NLoS) links [24]. WINNER channel models B1-LOS and B1-NLOS [24] are used to model the LoS and NLoS channels, respectively. MSs are connected to the BS with the least path loss. A network synchronised in time and frequency is assumed.

The traffic in the system is modeled as a burst of 100 protocol data units (PDUs) whose interarrival time is exponentially distributed. A PDU of 112 bit is assumed, which is the smallest unit of data that can be transmitted in one chunk. The average offered load per user L_u is adjusted by the interburst duration. It is considered that the arrival times for different users are independent. The maximum number of chunks that a user can be assigned in a given slot is the total number of available chunks in a frame. The simulation parameters are summarised in Table 1.

A 3/4-rate convolutional code and the SINR targets Γ_m for a given modulation scheme m are selected to attain a packet error ratio of 10^{-2} per PDU, given in Table 2. For non-adaptive modulation, we consider a 16-QAM constellation with $m = 4$ and a corresponding SINR target of $\Gamma_4 = 11.3$ dB. For link adaptation, the modulation schemes $m \in \mathcal{M}$ are chosen based on the achieved SINR targets Γ_m.

6. Results and Discussion

The performance of BB-OFDMA and the benchmark system (ASCA) are evaluated in terms of user and system throughput. User throughput is defined as the number of successfully received bits per user per unit time. A transmission is considered successful if the SINR target Γ is met at the receiver. The system throughput is defined as the aggregate throughput of all users per cell.

6.1. Collisions Based on Access Probability. The likelihood of achieving the SINR target during the initial access in contention is depicted in Figure 5 for $m = 4$ with $\Gamma_4 = 11.3$ dB, where m is the number of bits per symbol. The cell-edge region suffers from collisions (SINR target not met) both in the uplink (Figure 5(a)) and the downlink (Figure 5(b)). Decreasing the access probability p substantially reduces the occurrence of collisions, since the probability of simultaneous access of chunks in contention reduces (see Section 4.3). In the downlink, cell-edge users suffer from weaker desired signal power and at the same time experience strong CCI. Furthermore, the users located at the street crossings at $d = 115$ m are exposed to strong LoS interference from BSs in the perpendicular streets. In the uplink, however, these users cause CCI to the neighbouring cells; which may impact either users at the cell-edge or users closer to the intended BS.

TABLE 1: Simulation parameters.

Parameters	Value
Carrier centre frequency	3.95 GHz
System bandwidth B	89.84 MHz
No. of subcarriers (SCs)	1840
Subcarriers spacing Δf	48.8 kHz
OFDM symbols/frame $2n_{os}$	30
OFDM symbol duration T_{sym}	22.48 μs
Frame duration	0.6912 ms
No. of chunks/frame N_C	230
Chunk size $n_{sc} \times n_{os}$	8 (freq.) × 15 (time) = 120
PDU size	112 bits
Access probability p	0.3
No. of sectors/cell	1
No. of users/cell U	10
Tx power/chunk T^d	16.4 dBm
Antenna gain	0 dBi
Noise level/chunk N	−117.8 dBm
No. of snapshots	500
Snapshot duration	75 ms
User load L_u	30 Mbps

TABLE 2: Look up table for modulation scheme.

Modulation, No. of link PDUs per slot	Achieved SINR γ (dB)
No transmission $m = 0$	$-\infty < \gamma < 2.2$
BPSK $m = 1$	$2.2 \leq \gamma < 5.2$
QPSK $m = 2$	$5.2 \leq \gamma < 9.1$
Cross 8-QAM $m = 3$	$9.1 \leq \gamma < 11.3$
16-QAM $m = 4$	$11.3 \leq \gamma < 14.4$
Cross 32-QAM $m = 5$	$14.4 \leq \gamma < 16.6$
64-QAM $m = 6$	$16.6 \leq \gamma < 19.5$
Cross 128-QAM $m = 7$	$19.5 \leq \gamma < 22.5$
256-QAM $m = 8$	$22.5 \leq \gamma < \infty$

Consequently, the SINR target is met with less likelihood at street crossings and the cell edge in the downlink mode compared to the uplink mode.

6.2. Setting the Threshold for Fixed Power BB Signalling. The impact of the choice of interference threshold on the mean system throughput is shown in Figure 6 for fixed 16-QAM modulation with $m = 4$. It is seen that for lower values of I_{th}, the amount of allocated resources (Set $\mathcal{A}$) and the achieved throughput (Set $\mathcal{B}$) are approximately equal. This is because at low I_{th}, larger exclusion regions around active receivers are enforced. Thus, CCI is mitigated at the expense of spatial reuse. By increasing I_{th}, the system throughput gradually improves until the maximum is reached. However, increasing I_{th} introduces additional links that cause more CCI to the existing links. As a result, some of the links (mainly cell-edge users) are less likely to meet the SINR target. Although it is desirable to maximise the spectral
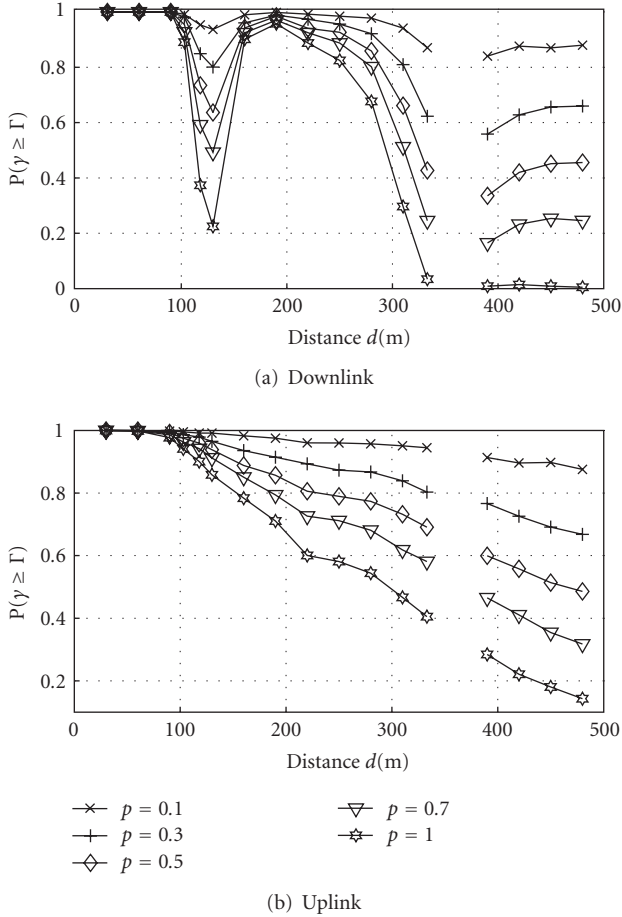
(a) Downlink

(b) Uplink

FIGURE 5: Probability of meeting the SINR target $\Gamma = 11.3$ dB in contention for different access probabilities p, as a function of the BS-MS distance d. At $d = 115$ m, links are exposed to strong LOS interference from cells in perpendicular streets, which causes collisions in the downlink, while at $d = 345$ m, the MSs are connected to BSs in a perpendicular street due to better channel gains.

efficiency, it may be necessary to maintain a fair distribution of resources to all users. Achieving a balance between maximising spectral efficiency and enhancing fairness is addressed in Section 6.3.

6.3. Impact of Interference Threshold on Fairness. Figure 7 shows the average user throughput versus distance d from the serving BS. It is observed that the performance of BB-OFDMA is sensitive to the chosen threshold I_{th}. The system throughput is maximised for $I_{th} = -75$ dBm in the downlink and for -85 dBm in the uplink (see Figure 6). However, these thresholds severely affect cell-edge user throughput. Increasing interference protection by lowering I_{th} enhances user throughput at the cell edge at the expense of system throughput. In the uplink (Figure 7(a)), the cell
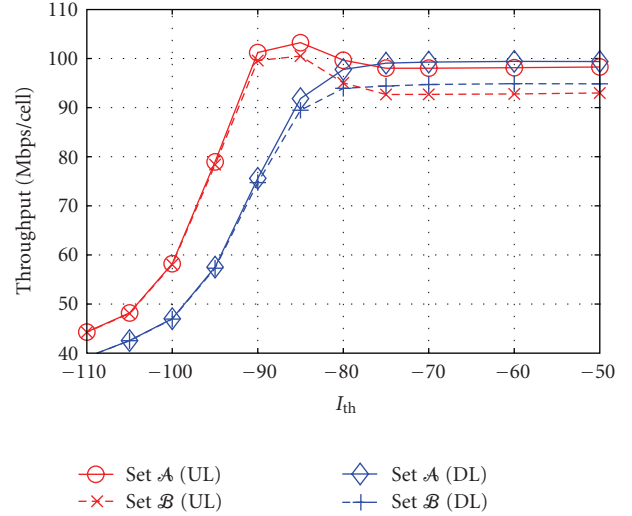
FIGURE 6: Mean system throughput versus I_{th} for BB-OFDMA with 16-QAM modulation using fixed BB transmit power. The mean system throughput is maximised for $I_{th} = -85$ dBm in the UL and $I_{th} = -75$ dBm in the DL.

edge throughput (measured at $d = 420$ m from the desired BS) improves from 1.5 Mbps ($I_{th} = -85$ dBm) to 3.08 Mbps ($I_{th} = -95$ dBm), an approximately onefold increase, whereas in the downlink (Figure 7(b)), user throughput increases from 267 kbps ($I_{th} = -75$ dBm) to 2.9 Mbps ($I_{th} = -90$ dBm), an approximately tenfold increase. At $d = 115$ m, MSs are exposed to LOS interference from BSs in perpendicular streets in the downlink. Consequently, high CCI compromises throughput for these users. In the uplink, MSs located at street crossings at $d = 115$ m transmit, so that these users are not exposed to LOS interference. Hence the uplink throughput of ASCA is not affected at $d = 115$ m. For BB-OFDMA, however, MSs located at street crossings are exposed to strong BB signals from BSs in perpendicular streets, which reduces the number of chunks such users can compete for, causing a drop of throughput for users located at street crossings.

Fairness is numerically quantified using Jain's fairness index (12). The cdf of the fairness distribution is presented in Figure 8(a) for the uplink and Figure 8(b) for the downlink. Applying the interference threshold that maximises system throughput, $I_{th} = -75$ dBm in the downlink and -85 dBm in the uplink, results in median fairness index of $F = 0.56$ and 0.66, respectively. Increasing the interference protection by lowering I_{th} improves fairness, as this enables cell-edge users to meet their SINR target. To this end, using $I_{th} = -95$ dBm in the uplink and -90 dBm in the downlink, approximately 22% of system throughput, is traded off for median fairness indices of $F \approx 0.72$. In the uplink, the median fairness index can be further improved to 0.78 by setting $I_{th} = -100$ dBm. However, the improved fairness significantly degrades system throughput (see Figure 6).

On the other hand, with BB-ITS, median fairness indices of ≈ 0.7 are achieved. The corresponding average uplink and downlink user throughputs at the cell edge amount to
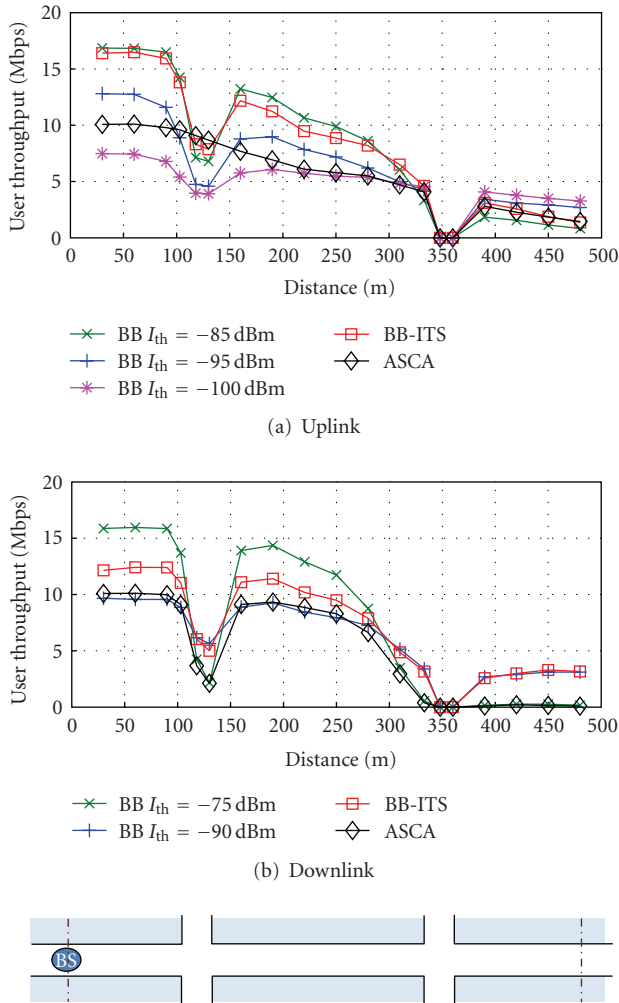
(a) Uplink

(b) Downlink

FIGURE 7: Mean user throughput versus distance from the serving BS, d, for BB-OFDMA with 16-QAM modulation for different interference thresholds I_{th}. For comparison, results for full-frequency reuse without interference protection termed ASCA are also included. Note that at $d = 115$ m, links are exposed to strong LOS interference (data in downlink, BB in uplink) from cells in perpendicular streets, which compromises throughput, while at $d = 345$ m, the MSs are connected to the BS in a perpendicular street due to better channel gains.
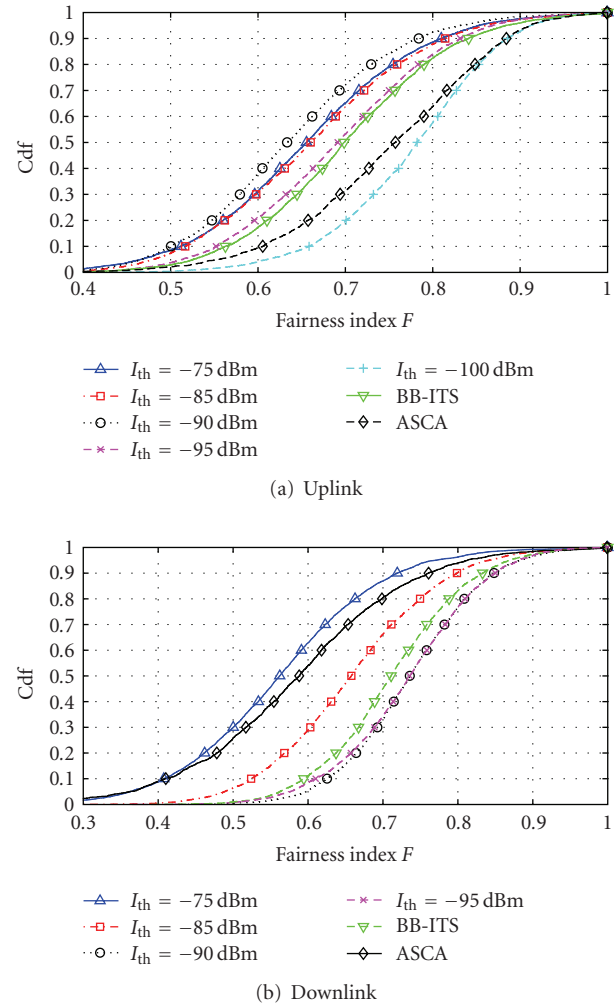

(a) Uplink

(b) Downlink

FIGURE 8: Cumulative distributive function (cdf) of Jain's fairness index (12) for BB-OFDMA compared to full-frequency reuse without interference avoidance (ASCA) both with 16-QAM modulation.

2.57 Mbps and 2.99 Mbps, respectively. The corresponding reduction in system throughput compared to the respective optimal thresholds with fixed power BB is only 1% in the uplink and 8% in the downlink. Note that BB-OFDMA with fixed BB power requires a 22% reduction in system throughput for a comparable performance at the cell edge. In light of this, BB-ITS results in a better tradeoff between system throughput and fairness.

For comparison, the median fairness resulting from ASCA is $F = 0.79$ in the uplink and 0.59 in the downlink. The corresponding average user throughputs at the cell edge are 2.278 Mbps and 208 kbps, respectively. This means that ASCA is more fair in the uplink compared to the downlink. The reason is that in the downlink cell-edge users are

exposed to high CCI, while in the uplink cell-edge users cause high CCI to adjacent cells. Hence the detrimental effects of interference on the uplink tend to be more equally distributed among all users.

6.4. Comparison between BB-OFDMA and ASCA. Figures 9(a)–9(d) depict the cumulative distribution function (cdf) of the user throughput and the system throughput. The results shown in Figures 9(a)-9(b) demonstrate that BB-enabled interference avoidance exhibits a gain in median system throughput of up to 50% compared to ASCA, both in uplink and downlink. Using a modulation format of $m = 4$ bits per symbol and a 3/4-rate convolutional code, the upper bound on system throughput achieved in an isolated cell (CCI free system) is 111.8 Mbps. With $I_{th} = -85$ dBm in the uplink and -75 dBm in the downlink, a median system throughput of about 90% and 85% of the upper bound (CCI free system) is achieved.

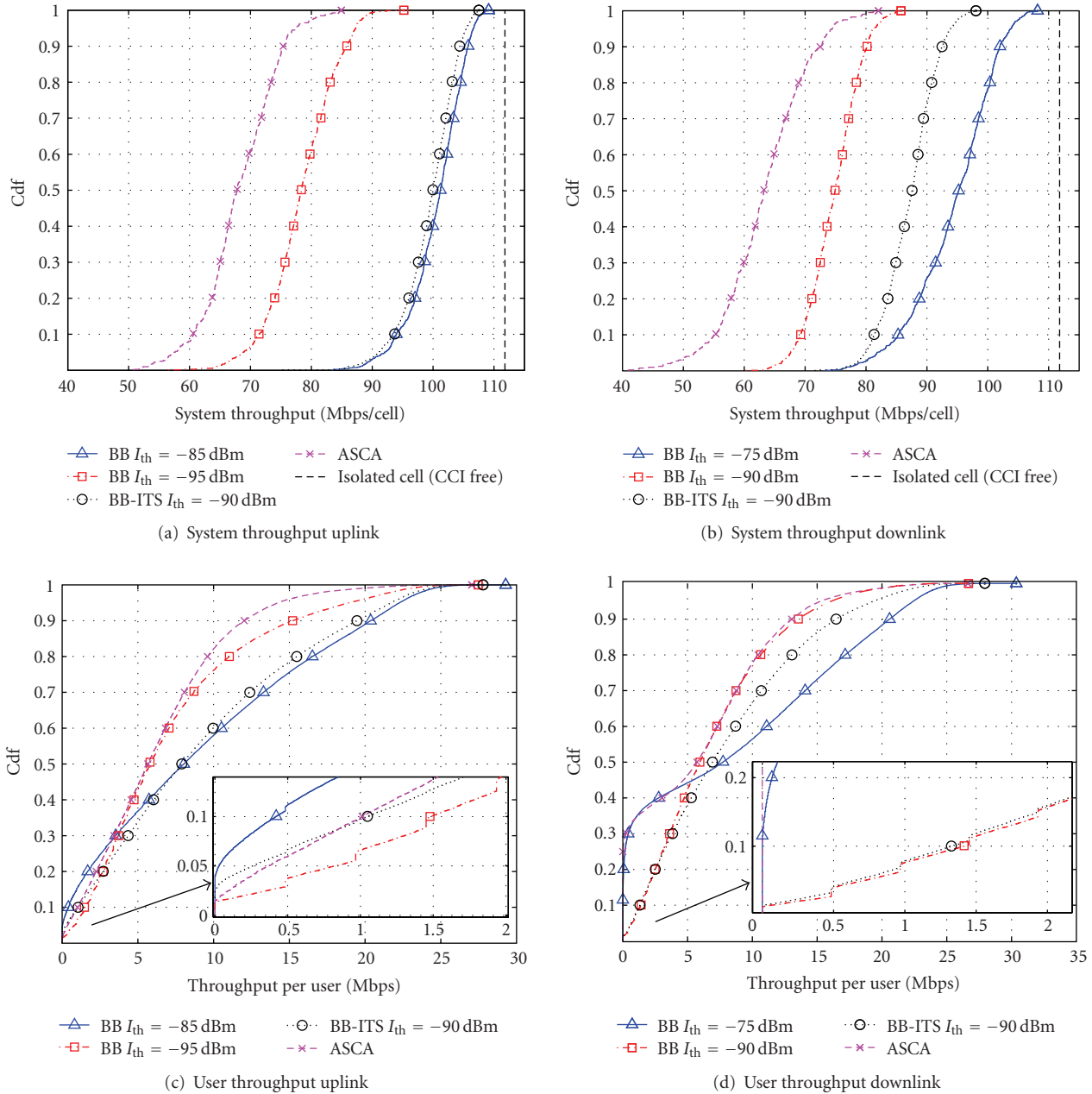Figures 9(c)-9(d) show the cdf of the user throughput for BB-OFDMA and ASCA. When fairness is the primary

FIGURE 9: Cumulative distributive function (cdf) of system throughput and user throughput for BB-OFDMA with fixed BB power and BB-ITS. The performance for full-frequency reuse without interference protection termed ASCA is included for comparison. BB-ITS results in a favourable tradeoff between fairness and system throughput both in uplink and downlink.

concern, $I_{th} = -95$ dBm in the uplink and $I_{th} = -90$ dBm in the downlink are preferable. Then the 10%-ile of the achieved user throughput amounts to 1.48 Mbps in the uplink (see Figure 9(c)) and 1.42 Mbps in the downlink (see Figure 9(d)). In contrast, ASCA fails to deliver any downlink throughput to more than 20% of the users. In the uplink, the 10%-ile of the user throughput of BB-OFDMA is improved by 40% compared to ASCA. With these uplink and downlink thresholds of $I_{th} = -95$ dBm and -90 dBm, the median system throughput of BB-OFDMA is still 15% and 18% higher than that achieved with ASCA (see Figures 9(a)-9(b)).

The results of BB-OFDMA with variable BB power, termed BB-ITS, are also included in Figures 9(a)–9(d). With BB-ITS, the lower 10%-ile of user throughput achieved is 1.04 Mbps in uplink and 1.416 Mbps in downlink (see Figures 9(c)-9(d)), at a modest degradation in system throughput (see Figures 9(a)-9(b)) compared to BB-OFDMA with fixed threshold that maximises the respective system throughput. BB-ITS, therefore, not only avoids the need for tuning the interference threshold so as to match a certain interference scenario (e.g., in uplink or downlink), but
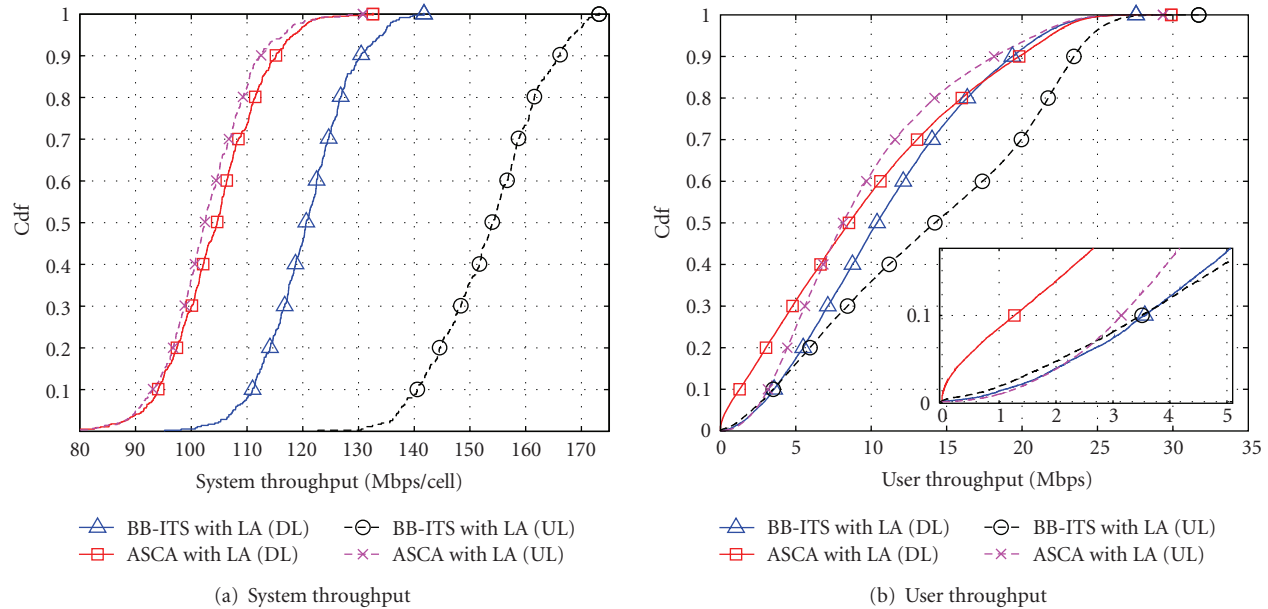
(a) System throughput

(b) User throughput

FIGURE 10: Cdfs of system and user throughputs for BB-ITS and ASCA with LA. In the DL, the users that are located at the cell-edge benefit whereas in the UL the users that are located closer to their desired BS benefit.

also achieves a preferable compromise between maximising system throughput and maintaining fairness.

6.5. Link Adaptation with BB-Signalling. Figures 10(a)-10(b) compare the system and user throughput achieved by performing link adaptation (LA) with BB-ITS and ASCA. Both BB-ITS and ASCA utilise the same link adaptation algorithm presented in Section 4.7; the only difference is that for ASCA interference protection is omitted. The results shown in Figure 10(a) reveal that BB-ITS with link adaptation attains an improvement of 50% (uplink) and 13% (downlink) in median system throughput compared to ASCA with link adaptation. Furthermore, Figure 10(b) shows that the BB-ITS outperforms ASCA by a factor of 2.75 in terms of the lower 10%-ile of the downlink user throughput. On the other hand, the cell-edge user throughput of BB-ITS and ASCA in the UL is comparable, while significant improvements of up to 70% are observed for higher percentiles of the user throughput in Figure 10(b).

By performing link adaptation with BB-ITS, the cell-edge users benefit in the downlink, whereas the users that are closer to their desired BS benefit in the uplink. The reason for this opposite trend for the uplink and the downlink is elaborated in the following. Due to the specific point-to-multipoint structure in the downlink, the CCI observed by the cell-edge users is dominated by the interference originating from the closest BS. When a chunk is assigned to a cell-edge user in the downlink, interference tolerance signalling enforces that this chunk cannot be spatially reused by the closest BS in an adjacent cell. By ensuring that, this dominant interferer does not access this chunk, the achieved SINR is greatly improved, potentially enough to meet the higher SINR target(s), thus allowing for the higher-order modulation schemes. In the uplink, on the other hand, the

chunks assigned to the cell-edge users are more likely to be reused in the adjacent cells due to the distributed location of the MSs transmitters (see Section 4.5). Consequently, it is less likely that a more spectrally efficient modulation scheme can be used by the cell-edge users. Furthermore, in the uplink, the distance between the MSs (transmitters) and the victim BSs (receivers) in neighbouring cells is larger for the cell-centre MSs than the cell-edge users. Hence the cell-centre users are more likely to be located outside the exclusion range of BSs receivers (BB transmitters). This results in a larger number of chunks that are available to be spatially reused for the cell-centre users. Lastly, the cell-centre users also benefit from higher SINRs as a result of which throughput is particularly boosted by performing link adaptation.

7. Conclusions

In this paper, the busy signal concept for decentralised and self-organised interference aware medium access has been applied to OFDMA-TDD systems operated in Manhattan grid deployment scenarios. An exclusion zone around victim receivers is established by means of receiver feedback in the form of time-multiplexed busy bursts (BBs), wherein no active transmitter from an adjacent cell may be located. BB enabled interference avoidance exhibits impressive gains in system and user throughputs compared to the benchmark system, with full-frequency reuse without interference avoidance, both in the uplink and the downlink. The impact of the BB specific threshold parameter that controls the interference imposed on coexisting links in neighbouring cells has been studied.

By adjusting this threshold parameter, the system benefits from flexible operation of either achieving high system throughput or enhanced fairness in terms of cell-edge

user throughput. A onefold (uplink) and tenfold (downlink) improvement in average cell-edge user throughput is achieved at a reduction in system throughput of about 22% ($\approx$20 Mbps/cell) in both cases. BB-enabled interference avoidance is therefore particularly powerful in enhancing downlink cell-edge user throughput, since in the downlink high interference is coupled with low-desired signal levels, resulting in poor average SINRs at the cell edge. In the uplink, on the other hand, cell-edge users cause high CCI, so that the detrimental effects of uplink interference are distributed more equally among all users, giving rise to *interference diversity*.

By allowing each receiver to signal the amount of interference it can tolerate, by using a variable busy burst power, an even better tradeoff between system throughput and fairness is achieved. Especially in the downlink, a tenfold improvement has been achieved at the cost of only 8% reduction in maximum system throughput. Furthermore, this scheme also alleviates the need to adjust the BB threshold parameter. The latter property is particularly important for self-organising wireless networks, as the optimum choice of the BB threshold is sensitive to changes in the network topology, and may not be known *a priori*.

Finally, link adaptation has been combined with busy burst-enabled interference avoidance, where changes in the transmission format are implicitly signalled to the transmitter by virtue of a variable BB power. BB signalling with link adaptation attained a superior performance than the benchmark system with link adaptation, both in terms of system throughput and user throughput. Due to the particular interference scenario, the cell-edge users achieved larger gains in the downlink whereas the cell-centre users benefitted more in the uplink. Consequently, larger gains in system throughput in the uplink mode were achieved compared to the gains achieved in the downlink mode.

Acknowledgments

References

[1] IEEE802.11a-1999, "Wireless LAN Medium Access Control (MAC) and Physical Layer (PHY) specifications; High-Speed Physical Layer in the 5 GHz Band," IEEE Standard Institution, Piscataway, NJ, USA, 1999.

[2] ETSI EN 300 744 v1.5.1 (2004-06), "Digital Video Broadcasting (DVB); Framing Structure, Channel Coding and Modulation for Digital Terrestrial Television," European Telecommunications Standards Institute (ETSI), June 2004.

[3] 3rd Generation Partnership Project (3GPP), "Evolved Universal Terrestrial Radio Access (E-UTRA); Physical Channels and Modulation (Release 8)," Technical Specification Group Radio Access Network, 3GPP TS 36.211 V8.2.0, 3GPP March 2008.

[4] M. Sternad, T. Svensson, T. Ottosson, A. Ahlen, A. Svensson, and A. Brunstrom, "Towards Systems Beyond 3G Based on Adaptive OFDMA Transmission," *Proceedings of the IEEE*, vol. 95, no. 12, pp. 2432–2455, 2007.

[5] S.-E. Elayoubi, O. Ben Haddada, and B. Fourestie, "Performance evaluation of frequency planning schemes in OFDMA-based networks," *IEEE Transactions on Wireless Communications*, vol. 7, no. 5, part 1, pp. 1623–1633, 2008.

[6] M. C. Necker, "Local interference coordination in cellular OFDMA networks," in *Proceedings of the 66th IEEE Vehicular Technology Conference (VTC '07)*, pp. 1741–1746, Baltimore, Md, USA, September-October 2007.

[7] S. M. Heikkinen, H. Haas, and G. J. R. Povey, "Investigation of adjacent channel interference in UTRA-TDD system," in *Proceedings of the IEE Colloquium on UMTS Terminals and Software Radio*, pp. 13/1–13/6, Glasgow, UK, April 1999.

[8] IST-4-027756 WINNER II, "D6.13.14 version 1.1 WINNER II System Concept Description," January 2008, http://www.ist-winner.org/WINNER2-Deliverables/D6.13.14 v1 .1.pdf.

[9] Z. Bharucha and H. Haas, "Application of the TDD underlay concept to home nodeB scenario," in *Proceedings of the 67th IEEE Vehicular Technology Conference (VTC '08)*, pp. 56–60, Singapore, May 2008.

[10] F. A. Tobagi and L. Kleinrock, "Packet switching in radio channels—part II: the hidden terminal problem in carrier sense multiple-access and the busy-tone solution," *IEEE Transactions on Communications*, vol. 23, no. 12, pp. 1417–1433, 1975.

[11] Z. J. Haas and J. Deng, "Dual busy tone multiple access (DBTMA)—a multiple access control scheme for ad hoc networks," *IEEE Transactions on Communications*, vol. 50, no. 6, pp. 975–985, 2002.

[12] R. Zhao, B. Walke, and M. Einhaus, "Constructing efficient multi-hop mesh networks," in *Proceedings of the 30th Anniversary IEEE Conference on Local Computer Networks (LCN '05)*, pp. 166–173, Sydney, Australia, November 2005.

[13] P. E. Omiyi and H. Haas, "Improving time-slot allocation in 4th generation OFDM/TDMA TDD radio access networks with innovative channel-sensing," in *Proceedings of the IEEE International Conference on Communications (ICC '04)*, vol. 6, pp. 3133–3137, Paris, France, June 2004.

[14] P. Omiyi, H. Haas, and G. Auer, "Analysis of TDD cellular interference mitigation using busy-bursts," *IEEE Transactions on Wireless Communications*, vol. 6, no. 7, pp. 2721–2731, 2007.

[15] H. Haas, V. D. Nguyen, P. Omiyi, N. Nedev, and G. Auer, "Interference aware medium access in cellular OFDMA/TDD networks," in *Proceedings of the IEEE International Conference on Communications (ICC '06)*, vol. 4, pp. 1778–1783, Istanbul, Turkey, July 2006.

[16] B. Ghimire, H. Haas, and G. Auer, "Busy burst enabled interference avoidance in winner-TDD," in *Proceedings of the 18th IEEE International Symposium on Personal, Indoor and Mobile Radio Communications (PIMRC '07)*, pp. 1–5, Athens, Greece, September 2007.

[17] IST-4-027756 WINNER II, "D6.13.7 v1.00, WINNER II Test Scenarios and Calibration Cases Issue 2," December 2006, http://www.ist-winner.org/WINNER2-Deliverables/D6.13.7.pdf.

[18] H. Haas and S. McLaughlin, Eds., *Next Generation Mobile Access Technologies: Implementing TDD*, Cambridge University Press, Cambridge, UK, 2008.

[19] T. S. Rappaport, *Wireless Communications: Principles and Practice*, Prentice Hall, Upper Saddle River, NJ, USA, 2nd edition, 2001.

[20] W. Wang, T. Ottosson, M. Sternad, A. Ahlén, and A. Svensson, "Impact of multiuser diversity and channel variability on adaptive OFDM," in *Proceedings of the 58th IEEE Vehicular Technology Conference (VTC '03)*, vol. 1, pp. 547–551, Orlando, Fla, USA, October 2003.

[21] T. Bonald, "A score-based opportunistic scheduler for fading radio channels," in *Proceedings of the European Wireless Conference (EWC '04)*, pp. 283–292, Barcelona, Spain, February 2004.

[22] R. Jain, D. Chiu, and W. Hawe, "A quantitative measure of fairness and discrimination for resource allocation in shared computer systems," Tech. Rep. TR-301, DEC, Maynard, Mass, USA, 1984.

[23] P. Agyapong, H. Haas, A. Tyrrell, and G. Auer, "Interference tolerance signaling using TDD busy tone concept," in *Proceedings of the 65th IEEE Vehicular Technology Conference (VTC '07)*, pp. 2850–2854, Dublin, Ireland, April 2007.

[24] IST-4-027756 WINNER II, "D1.1.2 v1.2 WINNER II Channel Models," November 2007, http://www.ist-winner.org/WINNER2-Deliverables/D1.1.2v1 .1.pdf.